STING activation reverses lymphoma-mediated resistance to antibody immunotherapy

Lekh N Dahal[1], **Lang Dou**[1], **Khiyam Hussain**[1], **Rena Liu**[1], **Alexander Earley**[1], **Kerry L Cox**[1], **Salome Murinello**[2], **Ian Tracy**[3], **Francesco Forconi**[3], **Andrew J Steele**[3], **Patrick J Duriez**[3], **Diego Gomez-Nicola**[2], **Jessica L Teeling**[2], **Martin J Glennie**[1], **Mark S Cragg**[1,*], and **Stephen A Beers**[1,*]

[1]Antibody & Vaccine Group, Cancer Sciences Unit, Faculty of Medicine, University of Southampton, Southampton General Hospital, Southampton SO16 6YD, UK

[2]Centre for Biological Sciences, University of Southampton, Southampton General Hospital, Southampton SO16 6YD, UK

[3]Cancer Sciences Unit, Cancer Research UK and NIHR Experimental Cancer Medicine Centres, University of Southampton, Southampton General Hospital, Southampton SO16 6YD, UK

Abstract

Tumors routinely attract and co-opt macrophages to promote their growth, angiogenesis and metastasis. Macrophages are also the key effector cell for monoclonal antibody (mAb) therapies. Here we report that the tumor microenvironment creates an immunosuppressive signature on tumor-associated macrophages (TAM) which favors expression of inhibitory rather than activating Fcγ receptors (FcγR), thereby limiting the efficacy of mAb immunotherapy. We assessed a panel of TLR and STING agonists (a) for their ability to reprogram macrophages to a state optimal for mAb immunotherapy. Both STINGa and TLRa induced cytokine release, modulated FcγR expression and augmented mAb-mediated tumor cell phagocytosis in vitro. However, only STINGa reversed the suppressive FcγR profile in vivo, providing strong adjuvant effects to anti-CD20 mAb in murine models of lymphoma. Potent adjuvants like STINGa which can improve FcγR activatory:inhibitory (A:I) ratios on TAM are appealing candidates to reprogram TAM and curb tumor-mediated immunosuppression, thereby empowering mAb efficacy.

Keywords

TAM; Macrophage polarisation; STING; TLR; FcγR

Introduction

Tumors can suppress the innate and adaptive arms of the immune system through regulation of myeloid cells (1, 2). Central to this suppressive capacity is the regulation of macrophages. Macrophages that have differentiated through interaction with tumor cells play a key role in exerting local immunosuppression and promoting tumour metastasis, neoplastic invasion of ectopic tissue and angiogenesis (3). Although the description of macrophage activation is currently contentious, these tumor promoting macrophages have been proposed to be akin to IL-4/-13 stimulated, anti-inflammatory "M2" macrophages generated during wound-healing which orchestrate Th2 responses and promote tissue repair and remodelling (4). Polarisation of TAM towards an LPS/IFN-γ activated, inflammatory "M1" state provides the potential to arrest these tumor promoting activities and alleviate immunosuppression (5). Reagents capable of achieving this have the capacity to provide anti-tumor effects; particularly as an adjuvant to immunotherapy and are keenly sought in cancer therapy (6).

Toll-like receptor agonists (TLRa) are potent stimulators of innate immunity, acting as "danger" signals that elicit phenotypic, secretory and transcriptomic changes in macrophages consistent with immune activation (7, 8). Several studies have shown that TLRa can provide adjuvants effects in human cancers; TLR9a CpG was shown to be feasible, safe and powerful to induce objective clinical response in lymphoma patients (9) and TLR7a Imiquimod was effective in the treatment of vulvar intraepithelial neoplasia (10). Efficacy of TLRa in combination with monoclonal antibody (mAb) therapy in animal models has also been explored. Agonistic anti-CD40 mAb combined with Imiquimod induced a systemic anti-tumor CD8+ T cell and type I Interferon response, significantly delaying the growth of implanted tumors and prolonging animal survival in models of mesothelioma (11) and melanoma (12). In our own studies (13), we have shown that TLR3a Polyinosinic:polycytidylic acid (Poly I:C) augmented the agonistic activity of anti-CD40 mAb dependent upon the upregulation of activating Fc-gamma receptors (FcγR). Although TLRa based reagents have been investigated in combination with antibody immunotherapy in humans (14), and such studies have motivated ongoing trials, they are yet to be successfully translated into the clinic (15).

Cyclic dinucleotides are a new class of immune adjuvants being evaluated in preclinical studies and in an early phase clinical trial in patients with advanced/metastatic solid tumors (NCT02675439).They signal via stimulator of interferon genes (STING), which is crucial for sensing DNA viruses (16, 17). Cytosolic DNA activates STING, leading to phosphorylation of IRF3 via tank-binding kinase 1 (TBK1), and subsequent transcription of type I interferon genes (17–19). In vivo studies have shown that STING -/- or IRF3 -/- mice fail to prime T cells against tumor antigens and do not reject immunogenic tumors (20), emphasising a critical role for host STING in immune sensing of tumors through dendritic cell (DC) activation and T cell priming (21, 22).

Here we document a comprehensive analysis of the efficacy of STING and TLR agonists in promoting macrophage pro-inflammatory activation, and tumoricidal function in combination with mAb immunotherapy. Certain TLRa were highly potent at activating both human and murine macrophages and augmenting antibody dependent cellular phagocytosis

(ADCP) in vitro but did not elicit similar potency in murine in vivo models of normal and malignant B cell depletion. However, STINGa were potent both in vitro and in vivo, crucially reversing lymphoma-mediated immunosuppression and providing protection in tumor bearing mice where immunotherapy alone failed. STINGa but not TLRa were subsequently shown to effectively reverse the suppressive effects induced by the lymphoma on macrophage FcγR expression, the principal immune effector cells in vivo.

Materials and Methods

Clinical Samples and Ethics

Ethical approval was obtained by Southampton University Hospitals NHS Trust from Southampton and South West Hampshire Research Ethics Committee. Informed consent was provided in accordance with the Declaration of Helsinki. CLL samples were from Human Tissue Authority licensed University of Southampton, Cancer Sciences Unit Tissue Bank and leukocyte cones from Southampton General Hospital National Blood Service.

Animals

Mice were bred and maintained in local facilities and experiments approved by the local ethical committee under Home Office license PPL30/2964. Experiments conformed to the Animal Scientific Procedure Act (UK). hCD20Tg, γ chain -/- and FcγR null mice (23, 24) have been described with genotypes confirmed by PCR and/or flow cytometry.

In vivo B cell depletion (adoptive transfer) assays

Splenocytes from target hCD20Tg (T) and non-target (NT) wild-type (unless otherwise specified) mice were labelled with 5μM and 0.5μM CFSE (Invitrogen), respectively, mixed (1:1), and i.v injected into recipients (5-8 × 10^6 cells/mouse). Two doses of adjuvant [TLR1/2a Pam3CSK4: 10-100μg, TLR2/4a LPS: 10μg, TLR3a Poly I:C: 100μg, TR7/8a R848: 2.5μg, DMXAA: 400μg, Type I IFN: 10,000 IU] were administered at 24 and 48h i.p, followed by Ritm2a (25-50μg) or isotype control i.v. For BALB/c mice, DMXAA was administered only once (300μg at 24h). Spleen was harvested 16-20h after Ritm2a administration, splenocytes stained with anti-mouse CD19 APC (eBioscience) and assessed for T:NT ratio. IFNAR blocking mAb (Clone MAR1-5A3; Leinco) was given at 500μg i.p as indicated in the figure legend.

Generation and polarisation of hMDM and mBMDM

hMDM and mBMDM were generated as described (23, 25). For hMDM polarisation, cells were stimulated with TLRa or STINGa (Invivogen) for 48 hours: [LPS: 50ng/ml, recombinant human (rh) IFN-γ: 2ng/ml (Peprotech), rhIL-4: 10ng/ml (Peprotech), rhIL-13: 10ng/ml (Peprotech), TLR1/2: Pam3CSK4 0.1μg/ml, TLR3: Poly I:C 40 μg/ml, TLR4: Monophosphoryl Lipid A (MPLA): 5μg/ml, TLR5: Flagellin: 125 ng/ml, TLR7/8: R848 1μM, 2'2-, 2'3'-, 3'3'-cGAMPs: 10-50μg/ml; Type I IFN: 5-100ng/ml]. For polarisation of mBMDM, cells were stimulated with recombinant murine (rm) IFN-γ: 2ng/ml (Peprotech), rmIL-4: 10ng/ml (Peprotech), rmIL-13: 10ng/ml (Peprotech), and TLRa or STINGa overnight (similar concentration as in hMDM).

Phenotypic analysis of hMDM/mBMDM and calculation of FcγR activatory:inhibitory (A:I) ratio

Human and murine FcγR staining is described elsewhere (26). Fluorescently conjugated mAb were from BD Biosciences, AbDSerotec, eBioscience or made in-house. hMDM were stained with anti-human CD40 Alexafluor (AF)488 (Clone ChiLob 7/6), CD38 AF488 (Clone AT 13/5), both in-house, and CD11b PE (eBioscience). mBMDM/Splenocytes were stained with anti-mouse CD11b PE, Ly6C PerCpCy5.5, Ly6G PeCy7 (eBioscience), F4/80 APC (AbD Serotec). Samples were acquired on FACS calibur/canto II (BD Bioscience) and data analysed with FCS express (DeNovo Software). FcγR A:I ratio for hMDM was calculated as: MFI for FcγRI*FcγRIIA*FcγRIII/FcγRIIB (FcγRI*FcγRIII*FcγRIV/FcγRII for mBMDM) giving a value of x for NT macrophage. The results for each test condition were then divided by x so that unstimulated macrophages received a ratio of 1.

hMDM and mBMDM phagocytosis assay and phagocytic index

Phagocytosis assay was performed as described (23, 25). hCD20 transgenic murine B cells and human CLL cells were used as targets for mBMDM and hMDM respectively. Phagocytic index was calculated by dividing the percentage of phagocytic macrophages under the test condition by the percentage of phagocytic macrophages seen in the unstimulated condition.

ELISA

Supernatant from macrophage cultures was harvested and levels of cytokines (IFN-γ, TNF-α, IL-12p70 and IL-6) assessed by MSD V-Plex assay (Meso scale discovery) according to the manufacturer's instructions. Type I Interferons IFN-α and IFN-β were measured by ELISA kit (PBL assays science).

BCL$_1$ lymphoma model and therapy

On day 0, 8-12 week female WT or FcγR null BALB/c mice were injected in tail vein with 1×10^4 BCL$_1$ tumor cells. DMXAA (300μg) and anti-CD20 18B12 (200μg, produced in-house from patented published sequences) were administered as indicated in Figure 7A. Anti-CD8 antibody YTS169 (500μg, in-house) was injected i.p on day 0, 5, 10 and 14. Tumor bearing mice were culled humanely before reaching terminal endpoint.

Chemokine and cytokine gene expression

RNA was purified from mice spleen using Qiagen RNAeasy mini kit. 500ng RNA was used to synthesise cDNA using RT^2 First Strand Kit and gene expression was assessed using RT^2 Profiler PCR mouse cytokine and chemokine array kit (Qiagen).

Statistical analysis

Statistical analysis was performed using GraphPadPrism. To compare differences between the experimental groups, student's t test, Wilcoxon, paired or unpaired t test analyses were performed; Kaplan Meier curves were produced and analysed by Log rank (Mantel-Cox) test. A P-value <0·05 was considered significant at the 95% confidence interval. Stars denote significance as follows: *p < 0.05, **p < 0.01, ***p < 0.001, and ****p < 0.0001.

Results

Tumors can generate a suppressive microenvironment with a low FcγR A:I ratio on macrophages leading to mAb therapy resistance

To explore how tumors can regulate their microenvironment in vivo, we performed adoptive transfer experiments (24) in mice harbouring the syngeneic mouse lymphoma, BCL$_1$ (27). The ability of the anti-human CD20 mAb, Ritm2a to deplete adoptively transferred target human CD20 transgenic (hCD20 Tg) B cells was examined (24). Whereas depletion of target cells was efficient in mice lacking tumor, in mice implanted with even low numbers (1×10^4) of BCL$_1$ cells 9 days prior to mAb administration, depletion was completely abrogated (Fig. 1A). As the lymphoma cells themselves lack the hCD20 target and are not deleted in this system, this directly demonstrates the ability of the tumor cells to elicit an immunosuppressive microenvironment. Analysis of cytokine and chemokine gene expression showed that inoculation of tumor upregulated expression of IL-10 and IL-21 (Supplementary Fig S1A). IL-10 has previously been directly implicated as a major immunosuppressive component of BCL$_1$ lymphoma (28, 29) and IL-21 has recently been identified to induce B cells to produce IL-10 (30). Previously, we have shown that mice depleted of macrophages are unable to eliminate target B cells (24), implicating macrophages as the most probable cells affected by this suppressive tumor microenvironment. We and others have shown that FcγR expression profiles on these cells are important for determining mAb efficacy (24, 25, 31) Therefore, next we investigated the differences in FcγR expression and A:I ratio (32) induced on splenic macrophages following BCL$_1$ inoculation. Tumor became detectable in the spleen only after day 14 post inoculation (Fig. 1B) with numbers significantly correlating with spleen weight (Fig. 1C). Increasing tumor presence corresponded to a significant decrease in expression of the activatory FcγRs I and III on splenic macrophages. Over the same time-course FcγRIV was marginally elevated, whilst the inhibitory FcγRII first showed an initial (day 7), small reduction and was then rapidly and substantially upregulated, ~four fold (Fig. 1D). This resulted in an overall, statistically significant suppression of macrophage FcγR A:I ratio by day 14 (Fig. 1E) which persisted to day 21. Further evidence of the ability of the tumor to manipulate macrophage activation status was observed by measuring F4/80, CD40 and CD11b (Supplementary Fig S1B). These data illustrate the profound effects that the tumor can elicit on macrophage FcγR expression profiles and phenotypic markers culminating in a substantially lowered A:I ratio and resistance to antibody mediated target cell depletion (Fig. 1A); even when very few tumor cells were detectable (e.g. at day 7 and 14). Notably, and in accordance with their redundancy in mediating target cell clearance in the adoptive transfer model (Supplementary Fig. S1C-E), monocytes and neutrophils did not show such profound changes in their FcγR A:I ratios (Fig. 1E).

The inhibitory FcγRII has been previously shown to suppress antibody-mediated depletion (33). We therefore assessed the contribution of elevated FcγRII levels to the defective mAb depletion in our system. We found that FcγRII knockout mice harbouring BCL$_1$ lymphoma treated with anti-CD20 mAb demonstrated enhanced (~50%) deletion of target cells compared to WT mice (Fig 1F). These results show that a significant proportion, but not all

of the effects of the tumor immune suppression is due to elevations in FcγRII and that strategies to enhance FcγR A:I would likely augment mAb activity.

FcγR changes induced in murine bone marrow derived macrophages (mBMDM) by TLRa and STINGa

Having established that FcγR profiles and A:I ratios on TAM were the key determinants of mAb-mediated target cell deletion, we sought to identify suitable TLR and STING ligand reagents capable of modifying these properties. The majority of TLRa tested did not show any activity with mBMDM, either in terms of modulating FcγR expression (Fig. 2A), increasing the FcγR A:I ratio (Fig. 2B) or augmenting phagocytosis (Fig. 2C). The sole exception was TLR3a (Poly I:C) which typically showed an increase in FcγR A:I ratio coincident with an increase in phagocytosis (Fig. 2B and C). In contrast to TLRa, both human (2'2'-, 2'3'- and 3'3'- cGAMP) and murine (DMXAA) STINGa showed increases in expression of activating FcγRs I, III and IV with no changes in FcγRII (Fig. 2A), culminating in an increased FcγR A:I ratio (Fig. 2B), and significant increases in phagocytosis (Fig. 2C and Supplementary Fig. S2). Notably, we observed a correlation between phagocytic activity of macrophages with their FcγR A:I ratio (Fig. 2D, R^2=0.48, p=0.0041).

Stimulation of mBMDM with STINGa also induced potent type I Interferon-α and $-\beta$ responses, with TLR3a again being the only TLRa to induce the secretion of these cytokines (Fig. 2E).

Phenotypic and cytokine changes induced in human monocyte derived macrophage (hMDM) stimulated with TLRa or STINGa

We next examined whether our observations pertaining to mouse macrophages could be translated to human. We first established that hMDM stimulated with TLRa displayed changes in a range of phenotypic markers; CD40, CD80, CD14, MHCII, CD206 and CD11b that were akin to changes induced by LPS/IFN-γ treatment (Supplementary Fig S3). We then investigated responses to a broader panel of both TLR and STINGa for their ability to induce phenotypic changes in hMDM in relation to the representative markers CD40, CD38 and CD11b. CD40 and CD38 are considered markers of immune cell activation and are generally upregulated on macrophages following stimulation with LPS (34, 35). Accordingly, CD40 and CD38 were significantly upregulated in hMDM stimulated with LPS/IFN-γ and decreased following IL-4/-13 treatment. Although the integrin $\alpha_m\beta_2$ (CD11b) is generally considered a pan-macrophage marker, its expression was significantly decreased with LPS/IFN-γ and increased with IL-4/-13 (Fig. 3A and 3B).

hMDM stimulated with both TLRa and STINGa showed a profile resembling LPS/IFN-γ stimulated macrophages with significant increases in CD40 seen with TLRa -1/2, -4, -5 and -7/8 and STINGa 2'2'- and 2'3'- cGAMP. Likewise, TLRa -1/2 and STINGa 2'2'- and 2'3'-cGAMP resulted in increased CD38. Most TLRa resulted in decreased CD11b akin to LPS/IFN-γ treated macrophages, with significant changes seen with TLRa -1/2, -4 and -7/8. The other TLRa or STINGa induced subtle changes in those markers, which were reflective of steady-state, non-polarised macrophages, demonstrating that within the spectrum of

polarisation, macrophages stimulated with TLRa and STINGa mostly display an inflammatory LPS/IFN-γ activated profile (Fig. 3A and 3B).

Consistent with an activated pro-inflammatory profile, supernatant from hMDM stimulated with TLRa contained elevated IFN-γ, IL-6, IL-12p70 and TNF-α, comparable to supernatant from LPS/IFN-γ stimulated macrophages (Fig. 3C). However, such cytokine responses were not seen following stimulation with STINGa; instead supernatant from STINGa 2'2'- and 2'3'- cGAMP treated macrophages displayed a type I interferon cytokine profile with release of both IFN-α and IFN-β (Fig. 3D), thereby demonstrating a divergence in STING and TLR inflammatory signalling with respect to cytokine induction in human myeloid cells.

FcγR changes and phagocytic activity of hMDM stimulated with TLRa or STINGa

We subsequently examined the expression pattern of activating (FcγRI, -IIA, -III) and inhibitory (FcγRIIB) FcγR on hMDM stimulated with TLRa or STINGa (Fig. 4A); and calculated the A:I ratio (Fig. 4B). TLRa -1/2, -5 and -7/8 showed an increase in the expression of activating FcγRs and decrease in inhibitory FcγRIIB resulting in an increased A:I ratio (Fig. 4 A-B), similar to LPS/IFN-γ polarised macrophages. STINGa 2'2' and 2'3' - cGAMP also resulted in an increase in the expression of activatory receptors FcγRIIA and FcγRIII, and a decrease in FcγRIIB, resulting in a statistically significant increase in A:I ratio (Fig. 4B and Supplementary Fig. S4A). In contrast, we observed a decrease in A:I ratio with IL-4/-13 polarised macrophages, largely mediated through an upregulation in FcγRIIB.

The phenotypic changes, cytokine profile and FcγR changes of hMDM treated with TLRa and STINGa were indicative of pro-inflammatory tumoricidal effectors. We therefore assessed if these cells also displayed augmented functional activity in terms of their ability to phagocytose antibody-opsonised CLL cells (Fig. 4C and Supplementary Fig S4B). Macrophages incubated in the presence of IL-4/-13 showed a decrease in phagocytic index whilst LPS/IFN-γ stimulated macrophages maintained a lower or similar phagocytic profile compared to unstimulated macrophages, perhaps due to the induction of higher levels of F-actin via the IFN-γ-mediated mechanism involving PI3K reported previously (36). TLRa -1/2, -5 and -7/8 and all STINGa stimulated hMDM showed a significant increase in their ability to phagocytose CLL cells (Fig. 4C), correlating with their A:I ratios (Fig. 4D, R^2=0.34, p=0.0007). It is not clear whether the contrasting activities of TLR3a in hMDM and mBMDM, both in terms of ADCP and type I interferon production relate to differences in TLR signalling pathways in human and murine cells, but cell type and species specific responses to TLR3 stimulation in human and murine effector cells have been previously reported (37).

STINGa but not TLRa enhance mAb-mediated target B cell depletion in the presence of the tumor microenvironment

Having established the relative abilities of TLRa and STINGa to augment FcγR mediated cell depletion with both murine and human macrophages in vitro we sought to determine their efficacy in vivo. Consistent with our findings with mBMDM, amongst the panel of TLRa assessed, only TLR3a significantly increased the mAb-mediated depletion of target B

cells in adoptive transfer assays in vivo. ~40% of target B cells were deleted by Ritm2a alone, whereas in mice primed with TLR3a ~60% of target B cells were depleted following Ritm2a administration (Fig. 5A). Intriguingly, the TLRa 1/2 that was potent with hMDM in vitro failed to enhance target B cell depletion in mice in vivo and appeared to be inhibitory. We next investigated the differences in FcγR expression and A:I ratio induced on splenic macrophages following TLRa -1/2 and -3 treatment (Fig. 5B). No significant change in FcγR A:I ratio was observed in macrophages from TLR1/2a treated mice, whilst TLR3a induced a significant increase in FcγR A:I ratio, likely explaining the elevated depletion with this reagent.

Whilst TLR3a mediated a modest increase in the depletion of adoptively-transferred target B cells in these experiments, the murine STING ligand DMXAA mediated a dramatic ~90% depletion of target B cells in combination with Ritm2a (Fig. 5C). We also observed a statistically significant, four-fold increase in the FcγR A:I ratio on splenic macrophages of mice that were primed with DMXAA compared to naïve mice (Fig. 5D) demonstrating that amongst all reagents assessed, DMXAA was the most potent in both upregulating the A:I ratio and depleting target B cells.

The adoptive transfer experiments discussed above provided a robust model to study target B cell depletion in the absence of any complexity arising from a suppressive tumor microenvironment. However, when BCL_1 cells were inoculated into recipient mice 1 week prior to adoptive transfer, the most potent TLRa Poly I:C failed to induce mAb target cell deletion, whilst DMXAA retained its efficacy even in the presence of the tumor (Fig. 5E). This DMXAA effect on Ritm2a activity was an antibody Fc dependent process as FcR γ chain KO mice, devoid of activatory FcγRs, were unable to delete target B cells in the same setting (Fig. 5E). When splenic macrophages from TLR3a or DMXAA treated tumor bearing mice were assessed for FcγR changes, we found that DMXAA but not TLR3a was able to completely reverse the suppressive effect of the tumor on the macrophage FcγR A:I ratio (Fig. 5F). Hence, the observed changes in FcγR A:I ratios provide an explanation as to why TLR3a loses its efficacy in tumor bearing hosts but DMXAA retains its ability to enhance mAb mediated B cell depletion even within an immunosuppressive tumor microenvironment. We were also able to exclude that this augmented deletion of target cells in the presence of tumor microenvironment was the result of any direct cytotoxic effect of DMXAA, as the percentage of both tumor and non-tumor B cells retrieved 24 hours after DMXAA injection into BCL_1-bearing mice was equivalent to that of mice not treated with DMXAA (Fig. 5G). Notably, administration of DMXAA induced upregulation of type I IFN gene expression and also reduced expression of both IL-10 and IL-21 that were upregulated following inoculation of the tumor (Supplementary Fig S5).

Type I IFN elicits macrophage FcγR skewing and augments mAb target cell deletion

In both human and murine cells, STINGa induced type I IFN (Fig 2-3, S5). Type I IFN is a key downstream mediator of STING activation (18), and therefore we interrogated if type I IFN were also able to modulate FcγR A:I ratio changes and target B cell deletion. We found that in hMDM, type I IFN induced upregulation of FcγRIIA and III leading to an increase in A:I ratio and phagocytosis of target CLL cells, in a manner similar to that mediated by

STINGa (Fig 6A). Likewise, administration of type I IFN to mice led to a significant increase in splenic macrophage FcγR A:I ratio, mostly mediated by an increase in FcγRIV, as seen with DMXAA (Fig 6B). mBMDM incubated in the presence of type I IFN also phagocytosed target cells more effectively, with a phagocytic index comparable to STINGa treated mBMDM (Fig 6B). Furthermore, Ritm2a-mediated deletion of target B cells in adoptive transfer assays were also significantly enhanced in mice that were primed with type I IFN prior to mAb administration (Fig 6C). Most importantly, the target B cell deleting ability of DMXAA was completely abrogated in mice that received IFNAR blocking antibody, further strengthening the role of type I IFN in downstream mechanisms governing the STING-mediated effects (Fig 6D).

STINGa DMXAA enhances mAb immunotherapy in BCL$_1$ lymphoma in an FcγR-dependent manner

Finally, having established that STING activation was capable of overcoming a suppressive lymphoma microenvironment to delete normal B cells in a transplant system, we assessed if the same approach could provide effective deletion of the malignant B cells themselves in a therapy model. BCL$_1$ bearing mice were treated with anti-mouse CD20 mAb (18B12) (38) in the presence or absence of DMXAA as depicted in Fig. 7A. When we monitored FcγR modulation in the therapy model, we observed that the tumor substantially downregulated activatory FcγRI and caused a dramatic increase in the inhibitory FcγRII. Both of these changes were reversed by DMXAA, which also induced a four-fold increase in FcγRIII and IV (Fig. 7B); allowing DMXAA to reverse the A:I changes induced by the lymphoma microenvironment (Fig. 7C). This was reflected in the survival of experimental animals: anti-CD20 and DMXAA monotherapies produced modest therapeutic effects whereas 90% of mice that were primed with DMXAA prior to anti-CD20 administration were effectively cured, surviving for longer than 100 days (Fig. 7D). This significant enhancement in tumor protection over anti-CD20 (median survival 36 days; p<0.0001) or DMXAA alone (median survival 32 days; p<0.0001) produced by the combination therapy was lost when mice were devoid of FcγRs (FcγR-null; median survival 30 days; Fig. 7E) showing that modulation of FcγRs is crucial to the combination effect. In contrast, the induction of an adaptive cytotoxic CD8^{+} T cell response is not required as 100% of mice receiving the combination therapy following CD8^{+} T cell depletion were also cured (Fig. 7F).

Discussion

TAM are typically immunosuppressive and have the capacity to negatively impact on anti-cancer immunotherapy strategies. Although deletion of TAM could overcome this issue, it will also impede tumor cell clearance with direct targeting antibodies, which rely on macrophages for their mode of action (24, 31) and are an important component of lymphoma treatment. Therefore, an alternative approach to restrict or prevent tumor growth and yet retain or provide an increased capacity of the TAM to deliver immunotherapy treatments is highly desired (39).

Here we identify that lymphoma cells can elicit a microenvironment that is profoundly suppressive, leading to resistance to mAb-mediated deletion of target cells and therapy.

Lowering of the TAM FcγR A:I ratio was a cardinal feature of the immunosuppressive tumor microenvironment illustrated here, achieved through a reduction of the activating FcγR and elevation of the inhibitory FcγRII. Almost all mAb used in the clinic to date, with the exception of 'true blockers' such as anti-PD1, rely on appropriate FcγR engagement for their optimal therapeutic activity (40, 41). Recalibration of the FcγR expression profile and A:I ratio is proposed to be one of the most important mechanisms by which mAb function can be modified. Clearly, tipping the balance in favour of higher A:I ratios may be beneficial in cancer immunotherapy treatments employing direct targeting mAbs. With regards anti-CD20 mAb and lymphoma, these changes appear to be more important in the macrophage population, as both monocytes and neutrophils were relatively unaffected by the tumor.

We demonstrate that the majority of TLRa tested polarised hMDM towards an activated phenotype, including an enhanced FcγR A:I ratio, induced a broad, pro-inflammatory cytokine response, and augmented their mAb-mediated phagocytic activity; all parameters desirable for anti-tumor immunity and yet had more modest effects on mBMDMs. The reasons for this are currently unclear but may reflect established species-specific differences (37). Alternatively, these differences may be attributed to the alternative progenitors from which the macrophages were generated (i.e. peripheral blood monocytes versus bone marrow precursors). Conversely, STINGa elicited more reproducible changes in FcγR, and type I IFN production, in both hMDM and mBMDM, effectively augmenting ADCP and performed consistently in murine assays both in vitro and in vivo. FcγR modulation is likely to be an important mechanism behind the activity of STINGa in vivo as its activity was completely abrogated in γ chain -/- mice lacking activating FcγR. Furthermore, the enhanced B cell depleting activity induced by STINGa was directly correlated with an enhanced A:I ratio, both in non-tumor and tumor bearing adoptive transfer assays.

Following its engagement, STING stimulates the transcription of numerous innate immune genes, including type I IFN with the capacity to augment macrophage activation (42). Our observations here indicate that type I IFN, together with FcγR modulation, rather than classical myeloid pro-inflammatory cytokine production may play an important role in augmenting STINGa based mAb immunotherapy. This point is of interest as it is known that after engagement of certain cyclic and double-stranded DNA molecules, STING elicits its effects on macrophages in a manner different to, and apparently independently of, other DNA recognising receptors, such as TLR9 (17). Generation of similar responses in terms of FcγR modulation, A:I ratio changes, enhanced phagocytosis, in vivo deletion and the inability of STINGa to delete target cells in the presence of IFNAR blocking antibodies indicate that type I IFN largely govern the downstream effects of STING agonism observed here, which are conserved between mice and humans.

The ability of STINGa but not TLRa to eliminate malignant B cells in vivo mirrors how well they reverse the lower FcγR A:I ratio in the macrophage population. Previously, we have shown that the inhibitory FcγRIIB helps tumor cells to escape deletion by rituximab (43, 44). Here we observed a significant improvement in deletion of target B cells in FcγRII knockout mice harbouring lymphoma, which suggests that some but not all of the immune suppression mediated by the tumor is due to the upregulation of FcγRII on macrophages, and strengthens the hypothesis that target cell deletion is a composite function of FcγR A:I

ratio. Therefore, adjuvants, such as STINGa, capable of eliciting such FcγR A:I ratio changes can be exploited in mAb immunotherapy. Importantly, and in marked contrast to TLRa, we have also demonstrated a commonality of response to STING agonism between mouse and human macrophages strongly supporting the translational nature of our observations. Some studies have suggested that STINGa can directly eradicate malignant B cells and mediate tumor regression (45) or disrupt tumor vasculature (46) leading to tumor necrosis, but we did not observe any direct cytotoxic killing of tumor cells in our study. Although disruption of tumor vasculature has been observed in certain subcutaneously grown tumor models and endothelial cells may be directly affected by DMXAA, we and others (47) have established that DMXAA primarily acts to induce macrophage activation and modulation of intratumoral macrophage phenotype to augment immunotherapy. Presumably, the discrepancies are attributed to the type of STINGa, differences in dosing strategy and the models used in the studies.

A principal finding of our study was the impressive potency of STINGa in augmenting macrophage activation and mAb-mediated effector mechanisms both in vitro and in vivo. Although the STINGa DMXAA showed very impressive effects in the murine lymphoma model studied here, early human cancer trials using DMXAA failed (48). Subsequent studies revealed that this was due to an inability of DMXAA to activate human STING (49). Since then, novel STINGa capable of engaging human STING have been generated and demonstrated potent adjuvant effects in the radiotherapeutic management of pancreatic cancer (50) and we have, for the first time, demonstrated its efficacy in a lymphoma model in conjunction with immunotherapy, in a manner dependent on FcγR A:I ratio changes, and in a context where TLRa failed. Studies should now be directed to the development, selection and formulation of cyclic dinucleotide analogs specific to human STING which deliver enhanced pharmacokinetics and defined potency.

Supplementary Material

Refer to Web version on PubMed Central for supplementary material.

Acknowledgements

References

1. Gajewski TF, Schreiber H, Fu Y-X. Innate and adaptive immune cells in the tumor microenvironment. Nat Immunol. 2013; 14:1014–22. [PubMed: 24048123]
2. Gabrilovich DI, Ostrand-Rosenberg S, Bronte V. Coordinated regulation of myeloid cells by tumors. Nat Rev Immunol. 2012; 12:253–68. [PubMed: 22437938]
3. Qian BZ, Pollard JW. Macrophage diversity enhances tumor progression and metastasis. Cell. 2010; 141:39–51. [PubMed: 20371344]

4. Murray PJ, Allen JE, Biswas SK, Fisher EA, Gilroy DW, Goerdt S, et al. Macrophage activation and polarization: nomenclature and experimental guidelines. Immunity. 2014; 41:14–20. [PubMed: 25035950]

5. Gordon S, Pluddemann A, Martinez Estrada F. Macrophage heterogeneity in tissues: phenotypic diversity and functions. Immunol Rev. 2014; 262:36–55. [PubMed: 25319326]

6. Schultze JL. Reprogramming of macrophages--new opportunities for therapeutic targeting. Curr Opin Pharmacol. 2016; 26:10–5. [PubMed: 26426255]

7. Xue J, Schmidt SV, Sander J, Draffehn A, Krebs W, Quester I, et al. Transcriptome-based network analysis reveals a spectrum model of human macrophage activation. Immunity. 2014; 40:274–88. [PubMed: 24530056]

8. Gordon S, Martinez FO. Alternative activation of macrophages: mechanism and functions. Immunity. 2010; 32:593–604. [PubMed: 20510870]

9. Brody JD, Ai WZ, Czerwinski DK, Torchia JA, Levy M, Advani RH, et al. In situ vaccination with a TLR9 agonist induces systemic lymphoma regression: a phase I/II study. J Clin Oncol. 2010; 28:4324–32. [PubMed: 20697067]

10. van Seters M, van Beurden M, ten Kate FJ, Beckmann I, Ewing PC, Eijkemans MJ, et al. Treatment of vulvar intraepithelial neoplasia with topical imiquimod. N Engl J Med. 2008; 358:1465–73. [PubMed: 18385498]

11. Broomfield SA, van der Most RG, Prosser AC, Mahendran S, Tovey MG, Smyth MJ, et al. Locally administered TLR7 agonists drive systemic antitumor immune responses that are enhanced by anti-CD40 immunotherapy. J Immunol. 2009; 182:5217–24. [PubMed: 19380767]

12. Ahonen CL, Wasiuk A, Fuse S, Turk MJ, Ernstoff MS, Suriawinata AA, et al. Enhanced efficacy and reduced toxicity of multifactorial adjuvants compared with unitary adjuvants as cancer vaccines. Blood. 2008; 111:3116–25. [PubMed: 18202224]

13. White AL, Dou L, Chan HT, Field VL, Mockridge CI, Moss K, et al. Fcgamma receptor dependency of agonistic CD40 antibody in lymphoma therapy can be overcome through antibody multimerization. J Immunol. 2014; 193:1828–35. [PubMed: 25024386]

14. Friedberg JW, Kelly JL, Neuberg D, Peterson DR, Kutok JL, Salloum R, et al. Phase II study of a TLR-9 agonist (1018 ISS) with rituximab in patients with relapsed or refractory follicular lymphoma. Br J Haematol. 2009; 146:282–91. [PubMed: 19519691]

15. Leonard JP, Link BK, Emmanouilides C, Gregory SA, Weisdorf D, Andrey J, et al. Phase I trial of toll-like receptor 9 agonist PF-3512676 with and following rituximab in patients with recurrent indolent and aggressive non Hodgkin's lymphoma. Clin Cancer Res. 2007; 13:6168–74. [PubMed: 17947483]

16. Burdette DL, Monroe KM, Sotelo-Troha K, Iwig JS, Eckert B, Hyodo M, et al. STING is a direct innate immune sensor of cyclic di-GMP. Nature. 2011; 478:515–8. [PubMed: 21947006]

17. Ishikawa H, Barber GN. STING is an endoplasmic reticulum adaptor that facilitates innate immune signalling. Nature. 2008; 455:674–8. [PubMed: 18724357]

18. Sun L, Wu J, Du F, Chen X, Chen ZJ. Cyclic GMP-AMP synthase is a cytosolic DNA sensor that activates the type I interferon pathway. Science. 2013; 339:786–91. [PubMed: 23258413]

19. Wu J, Sun L, Chen X, Du F, Shi H, Chen C, et al. Cyclic GMP-AMP is an endogenous second messenger in innate immune signaling by cytosolic DNA. Science. 2013; 339:826–30. [PubMed: 23258412]

20. Woo SR, Fuertes MB, Corrales L, Spranger S, Furdyna MJ, Leung MY, et al. STING-dependent cytosolic DNA sensing mediates innate immune recognition of immunogenic tumors. Immunity. 2014; 41:830–42. [PubMed: 25517615]

21. Corrales L, Glickman LH, McWhirter SM, Kanne DB, Sivick KE, Katibah GE, et al. Direct Activation of STING in the Tumor Microenvironment Leads to Potent and Systemic Tumor Regression and Immunity. Cell Reports. 2015; 11:1018–30. [PubMed: 25959818]

22. Woo SR, Corrales L, Gajewski TF. The STING pathway and the T cell-inflamed tumor microenvironment. Trends Immunol. 2015; 36:250–6. [PubMed: 25758021]

23. Beers SA, Chan CH, James S, French RR, Attfield KE, Brennan CM, et al. Type II (tositumomab) anti-CD20 monoclonal antibody out performs type I (rituximab-like) reagents in B-cell depletion regardless of complement activation. Blood. 2008; 112:4170–7. [PubMed: 18583569]

24. Beers SA, French RR, Chan HT, Lim SH, Jarrett TC, Vidal RM, et al. Antigenic modulation limits the efficacy of anti-CD20 antibodies: implications for antibody selection. Blood. 2010; 115:5191–201. [PubMed: 20223920]

25. Tipton TR, Roghanian A, Oldham RJ, Carter MJ, Cox KL, Mockridge CI, et al. Antigenic modulation limits the effector cell mechanisms employed by type I anti-CD20 monoclonal antibodies. Blood. 2015; 125:1901–9. [PubMed: 25631769]

26. Tutt AL, James S, Laversin SA, Tipton TR, Ashton-Key M, French RR, et al. Development and Characterization of Monoclonal Antibodies Specific for Mouse and Human Fcgamma Receptors. J Immunol. 2015; 195:5503–16. [PubMed: 26512139]

27. Uhr JW, Tucker T, May RD, Siu H, Vitetta ES. Cancer dormancy: studies of the murine BCL1 lymphoma. Cancer Res. 1991; 51:5045s–53s. [PubMed: 1884380]

28. BitMansour A, Pop LM, Vitetta ES. The Role of Regulatory B Cell-Like Malignant Cells and Treg Cells in the Mouse Model of BCL1 Tumor Dormancy. PloS One. 2016; 11:e0167618. [PubMed: 27959896]

29. O'Garra A, Stapleton G, Dhar V, Pearce M, Schumacher J, Rugo H, et al. Production of cytokines by mouse B cells: B lymphomas and normal B cells produce interleukin 10. Int Immunol. 1990; 2:821–32. [PubMed: 1703785]

30. Yoshizaki A, Miyagaki T, DiLillo DJ, Matsushita T, Horikawa M, Kountikov EI, et al. Regulatory B cells control T-cell autoimmunity through IL-21-dependent cognate interactions. Nature. 2012; 491:264–8. [PubMed: 23064231]

31. Gul N, Babes L, Siegmund K, Korthouwer R, Bogels M, Braster R, et al. Macrophages eliminate circulating tumor cells after monoclonal antibody therapy. J Clin Invest. 2014; 124:812–23. [PubMed: 24430180]

32. Nimmerjahn F, Ravetch JV. Divergent immunoglobulin g subclass activity through selective Fc receptor binding. Science. 2005; 310:1510–2. [PubMed: 16322460]

33. Clynes RA, Towers TL, Presta LG, Ravetch JV. Inhibitory Fc receptors modulate in vivo cytotoxicity against tumor targets. Nat Med. 2000; 6:443–6. [PubMed: 10742152]

34. Vogel DY, Glim JE, Stavenuiter AW, Breur M, Heijnen P, Amor S, et al. Human macrophage polarization in vitro: maturation and activation methods compared. Immunobiology. 2014; 219:695–703. [PubMed: 24916404]

35. Lee CU, Song EK, Yoo CH, Kwak YK, Han MK. Lipopolysaccharide induces CD38 expression and solubilization in J774 macrophage cells. Molecules and cells. 2012; 34:573–6. [PubMed: 23184288]

36. Frausto-Del-Rio D, Soto-Cruz I, Garay-Canales C, Ambriz X, Soldevila G, Carretero-Ortega J, et al. Interferon gamma induces actin polymerization, Rac1 activation and down regulates phagocytosis in human monocytic cells. Cytokine. 2012; 57:158–68. [PubMed: 22137120]

37. Lundberg AM, Drexler SK, Monaco C, Williams LM, Sacre SM, Feldmann M, et al. Key differences in TLR3/poly I:C signaling and cytokine induction by human primary cells: a phenomenon absent from murine cell systems. Blood. 2007; 110:3245–52. [PubMed: 17660379]

38. Brezinsky SC, Chiang GG, Szilvasi A, Mohan S, Shapiro RI, MacLean A, et al. A simple method for enriching populations of transfected CHO cells for cells of higher specific productivity. J Immunol Methods. 2003; 277:141–55. [PubMed: 12799047]

39. Ginhoux F, Schultze JL, Murray PJ, Ochando J, Biswas SK. New insights into the multidimensional concept of macrophage ontogeny, activation and function. Nat Immunol. 2016; 17:34–40. [PubMed: 26681460]

40. Dahal LN, Roghanian A, Beers SA, Cragg MS. FcgammaR requirements leading to successful immunotherapy. Immunol Rev. 2015; 268:104–22. [PubMed: 26497516]

41. Dahan R, Sega E, Engelhardt J, Selby M, Korman AJ, Ravetch JV. FcgammaRs Modulate the Anti-tumor Activity of Antibodies Targeting the PD-1/PD-L1 Axis. Cancer cell. 2015; 28:285–95. [PubMed: 26373277]

42. Hartlova A, Erttmann SF, Raffi FA, Schmalz AM, Resch U, Anugula S, et al. DNA damage primes the type I interferon system via the cytosolic DNA sensor STING to promote anti-microbial innate immunity. Immunity. 2015; 42:332–43. [PubMed: 25692705]

43. Lim SH, Vaughan AT, Ashton-Key M, Williams EL, Dixon SV, Chan HT, et al. Fc gamma receptor IIb on target B cells promotes rituximab internalization and reduces clinical efficacy. Blood. 2011; 118:2530–40. [PubMed: 21768293]

44. Roghanian A, Teige I, Martensson L, Cox KL, Kovacek M, Ljungars A, et al. Antagonistic human FcgammaRIIB (CD32B) antibodies have anti-tumor activity and overcome resistance to antibody therapy in vivo. Cancer cell. 2015; 27:473–88. [PubMed: 25873171]

45. Tang CH, Zundell JA, Ranatunga S, Lin C, Nefedova Y, Del Valle JR, et al. Agonist-Mediated Activation of STING Induces Apoptosis in Malignant B Cells. Cancer Res. 2016; 76:2137–52. [PubMed: 26951929]

46. Downey CM, Aghaei M, Schwendener RA, Jirik FR. DMXAA causes tumor site-specific vascular disruption in murine non-small cell lung cancer, and like the endogenous non-canonical cyclic dinucleotide STING agonist, 2'3'-cGAMP, induces M2 macrophage repolarization. PloS One. 2014; 9:e99988. [PubMed: 24940883]

47. Fridlender ZG, Jassar A, Mishalian I, Wang LC, Kapoor V, Cheng G, et al. Using macrophage activation to augment immunotherapy of established tumors. Br J Cancer. 2013; 108:1288–97. [PubMed: 23481183]

48. Lara PN Jr, Douillard JY, Nakagawa K, von Pawel J, McKeage MJ, Albert I, et al. Randomized phase III placebo-controlled trial of carboplatin and paclitaxel with or without the vascular disrupting agent vadimezan (ASA404) in advanced non-small-cell lung cancer. J Clin Oncol. 2011; 29:2965–71. [PubMed: 21709202]

49. Conlon J, Burdette DL, Sharma S, Bhat N, Thompson M, Jiang Z, et al. Mouse, but not human STING, binds and signals in response to the vascular disrupting agent 5,6-dimethylxanthenone-4-acetic acid. J Immunol. 2013; 190:5216–25. [PubMed: 23585680]

50. Baird JR, Friedman D, Cottam B, Dubensky TW Jr, Kanne DB, Bambina S, et al. Radiotherapy Combined with Novel STING-Targeting Oligonucleotides Results in Regression of Established Tumors. Cancer Res. 2016; 76:50–61. [PubMed: 26567136]
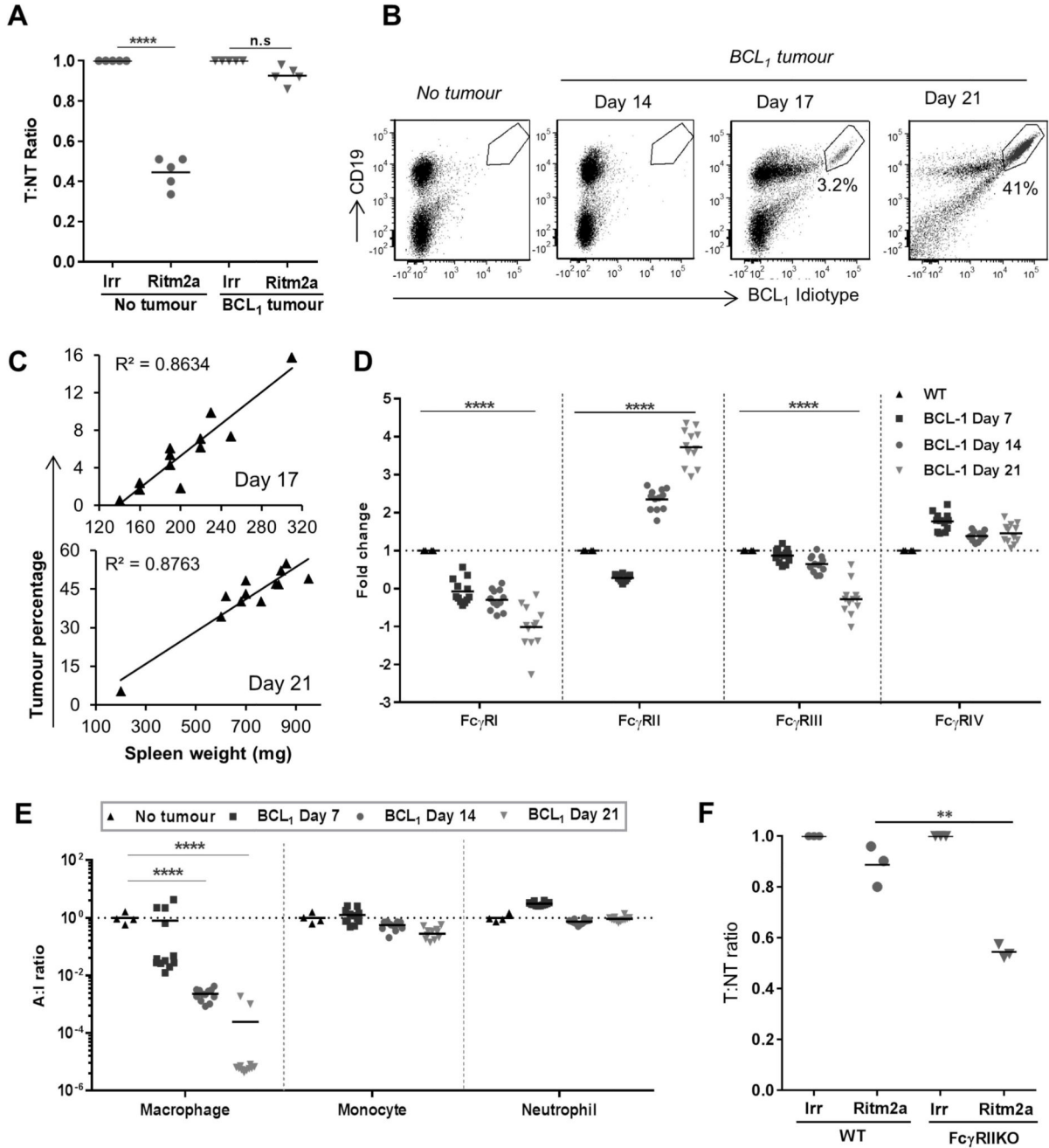
Figure 1. BCL$_1$ lymphoma generates a profoundly immunosuppressive tumor microenvironment.

(A) WT BALB/c mice were implanted with BCL$_1$ lymphoma cells 1 week prior to transfer of target (T) hCD20Tg B cells and non-Tg non-target (NT) B-cells. Mice were then treated with Ritm2a 2 days later and spleens harvested the following day and assessed for T:NT ratio (n=5-6, Wilcoxon test). **(B)** WT BALB/c mice were implanted with BCL$_1$ lymphoma and the number of tumor cells in the spleen quantitated by flow cytometry. **(C)** Correlation between spleen weight and tumor percentage in the spleen. **(D)** Fold change in macrophage

FcγR expression and **(E)** A:I ratio on splenic macrophages, monocytes and neutrophils (n=12, student's t test). **(F)** Adoptive transfer as in A, in BCL$_1$ lymphoma bearing WT vs FcγRII KO BALB/c recipient mice with hCD20TgxFcγRII KO B cells as target (T) and FcγRIIKO B cells as non-targets (NT).
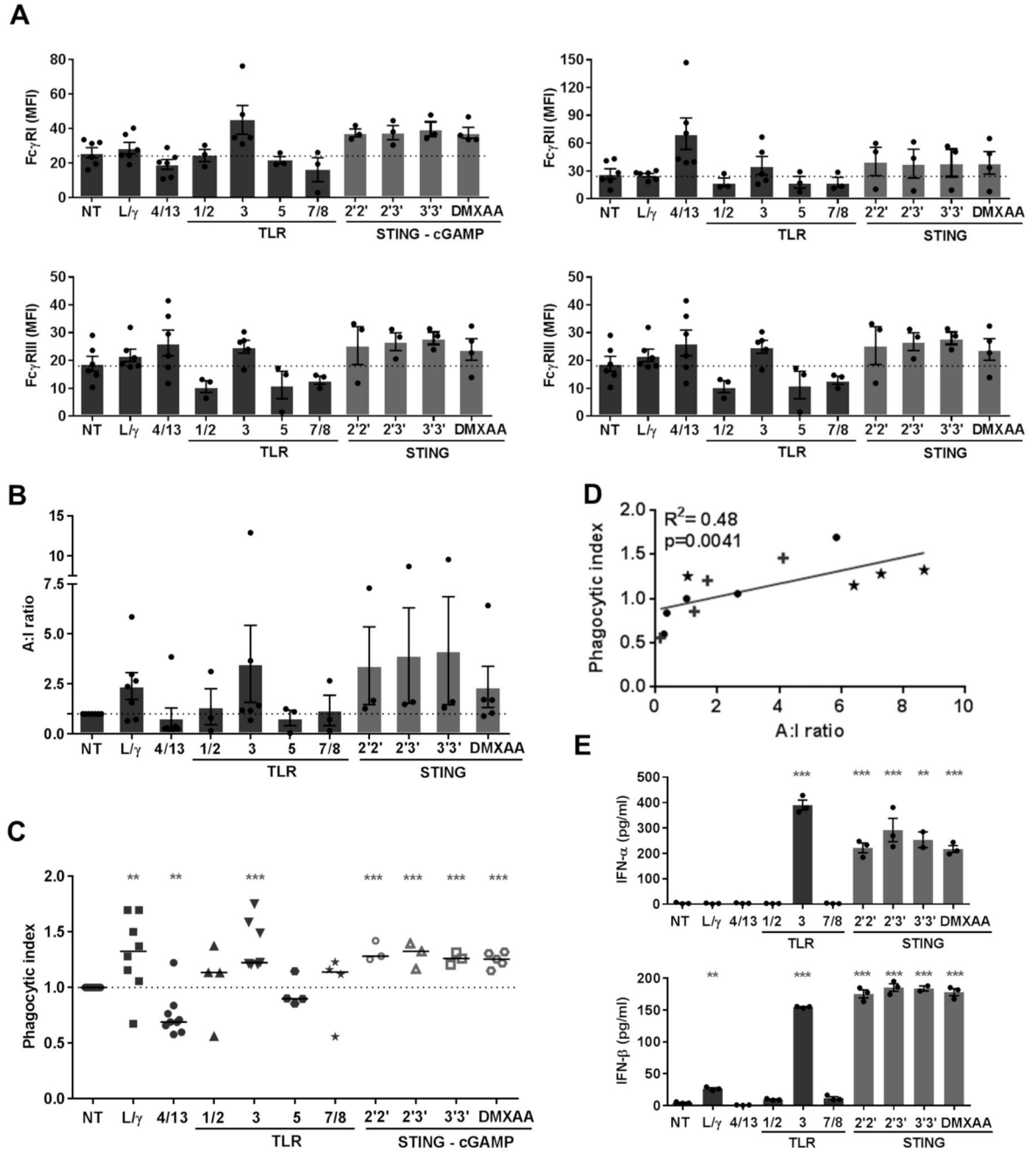
Figure 2. Phenotypic and functional changes induced by TLRa or STINGa on mBMDM.
(**A**) FcγR expression (**B**) A:I ratio and (**C**) phagocytic index of mBMDM following stimulation with LPS/IFN-γ, (L/γ), IL-4/-13 (4/13), TLRa or STINGa (n=3-6, error bar ±SEM, student's t-test). (**D**) Correlation between A:I ratio and phagocytic index (★ STINGa mBMDM, + TLRa mBMDM, ● NT, 4/13 and L/γ mBMDM, analysed by linear regression). (**E**) mBMDM supernatant assessed for IFN-α and IFN-β (n=3, error bars±SEM, student's t-test)
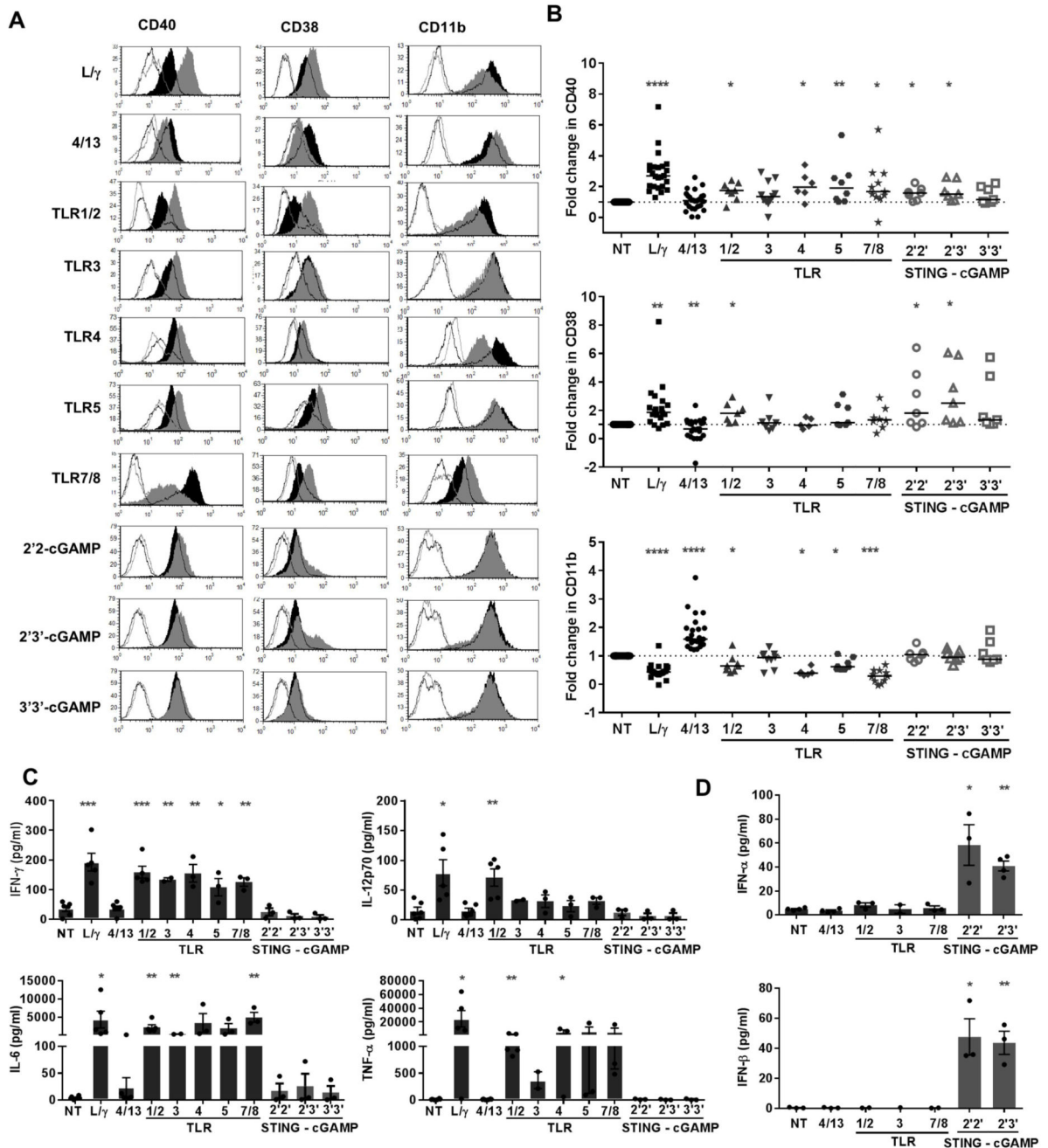
Figure 3. Phenotypic changes and cytokine profile of hMDM stimulated with TLRa or STINGa.
(**A**) FcγR changes [Open black histogram: Iso ctrl for NT macrophage, Filled black histogram: surface marker on NT macrophage, Open grey histogram: Iso ctrl for TLRa/STINGa treated macrophage, Filled grey histogram:surface marker for TLRa/STINGa treated macrophage], (**B**) Fold change in CD40, CD38 and CD11b following stimulation with LPS/IFN-γ (L/γ) IL-4/-13 (4/13), TLRa or STINGa (n=6-25, Wilcoxon test). (**C and D**) Macrophage supernatant assessed for cytokines by ELISA (error bars±SEM, student's t-test).
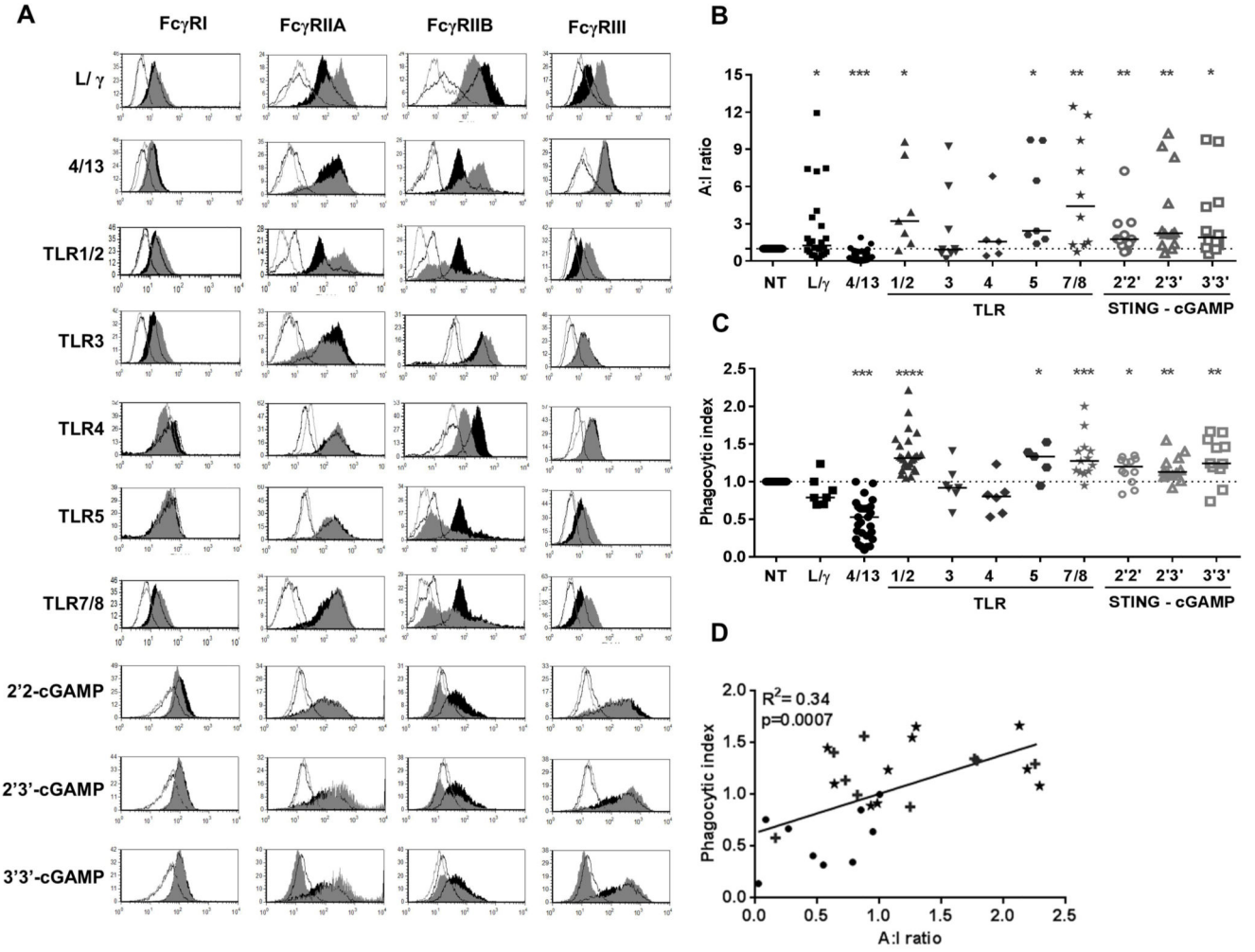
Figure 4. FcγR expression and ADCP of tumor cells following stimulation of hMDM with TLRa or STINGa.

(A) FcγR changes [Open black histogram: Iso ctrl for NT macrophage, Filled black histogram: Expression of FcγR on NT macrophage, Open grey histogram: Iso ctrl for TLRa/STINGa treated macrophage, Filled grey histogram: Expression of FcγR on TLRa/STINGa treated macrophage], **B)** A:I ratio and **C)** phagocytic index of hMDM following stimulation with LPS/IFN-γ (L/γ) IL-4/-13 (4/13), TLRa or STINGa. (n=6-25; Wilcoxon test) **(D)** Correlation between A:I ratio and phagocytic index (★ STINGa hMDM, + TLRa hMDM, ● NT, 4/13 and L/γ hMDM, analysed by linear regression).
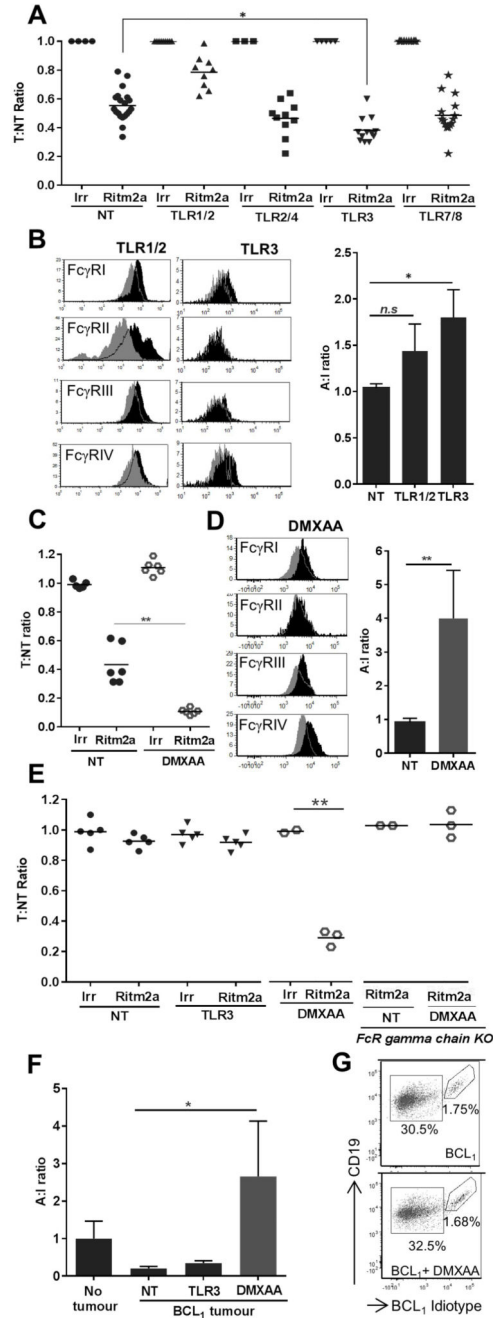
Figure 5. Effect of TLRa and murine STINGa on mAb-mediated target B cell depletion in vivo.
(**A**) WT C57BL/6 mice were primed with TLRa -1/2, -2/4, -3 or -7/8 after adoptive transfer and assessed for T:NT ratio as in Figure 1A (n=9-20, Wilcoxon test). (**B**) Representative histograms showing changes in FcγR expression (grey: naïve mice, black: TLRa treated mice) and A:I ratio of splenic macrophages. (**C**) Adoptive transfer as in A with STINGa DMXAA prior to Ritm2a treatment (n=6, Wilcoxon test). (**D**) Representative histograms showing changes in FcγR expression (grey: naïve mice, black: DMXAA treated mice) and A:I ratio in splenic macrophages from WT C57BL/6 mice that were primed with DMXAA.

(E) Adoptive transfer in WT BALB/c or FcR γ chain -/- mice conducted a week after implantation of BCL_1 cells. Mice were treated with TLR3a or DMXAA prior to Ritm2a administration and T:NT ratio determined (n=2-5, Wilcoxon test). (F) A:I ratio of splenic macrophages from E, (G) Flow cytometric analysis of the spleen of BALB/c mice that were treated with DMXAA 15 days after inoculation with BCL_1 cells.
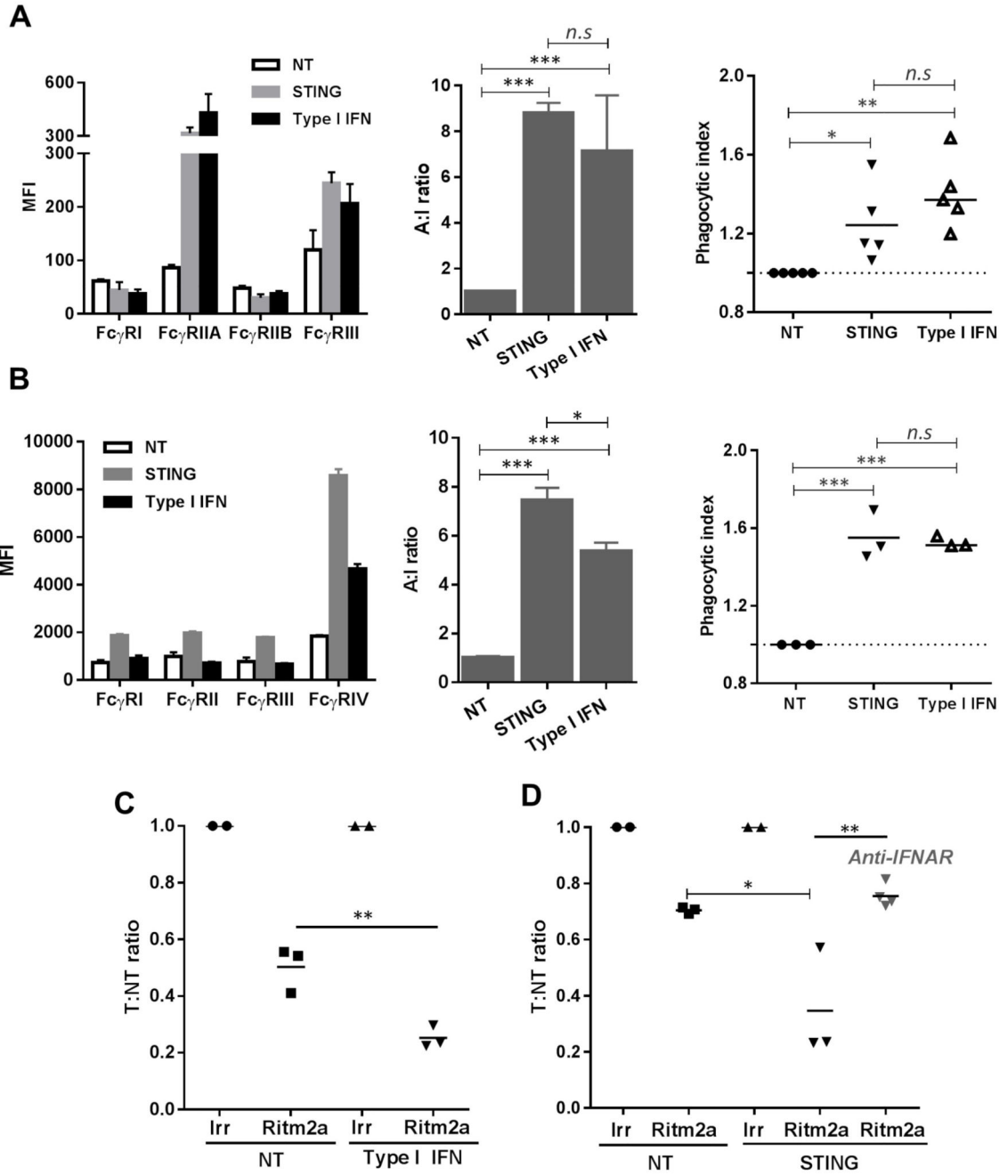
Figure 6. STINGa mediated effects can be recapitulated by type I IFN and prevented by IFNAR blocking

(**A**) FcγR expression (left), A:I ratio (middle) and phagocytic index (right) of hMDM stimulated with STINGa 2'3'-cGAMP or IFN-α (n=3, error bar±SEM). (**B**) FcγR expression (left), A:I ratio (middle) of splenic macrophages from WT C57BL/6 mice injected with murine STINGa DMXAA or IFN-α and mBMDM phagocytic index (right). (**C**). WT C57BL/6 mice were primed with IFN-α after adoptive transfer as in 1A and T:NT ratio determined (**D**) Adoptive transfer in WT C57BL/6 mice primed with DMXAA, and

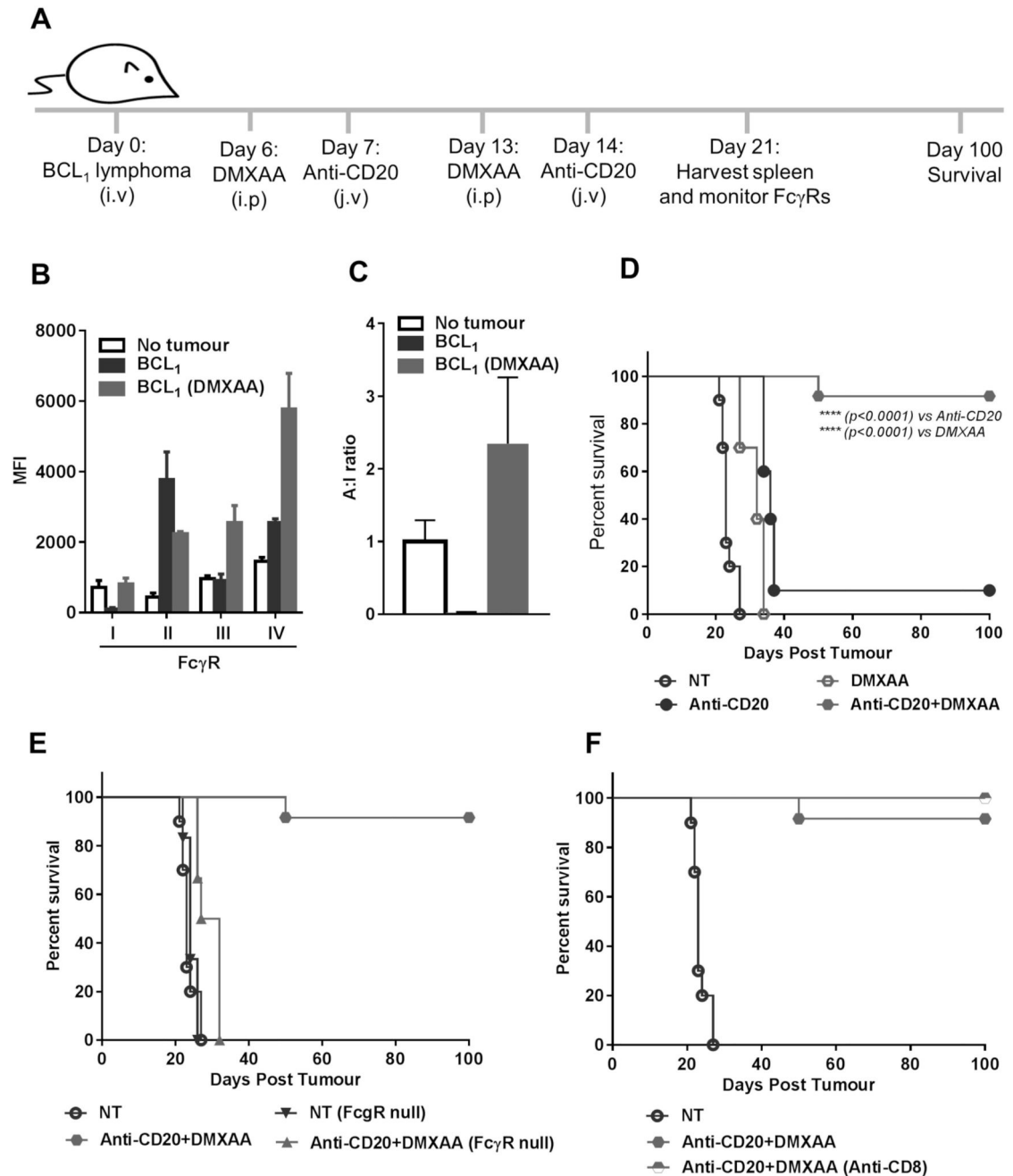receiving anti-IFNAR (day -1,0 and 1, adoptive transfer on day 0; analysed by student's t test).

Figure 7. STINGa enhances mAb immunotherapy in BCL$_1$ lymphoma in an FcγR dependent manner.
(**A**) Experimental plan to assess the effect of DMXAA on mAb immunotherapy. (**B**) FcγR expression and (**C**) A:I ratio on splenic macrophages on day 21 after BCL$_1$ inoculation (error bar±SEM). (**D**) Kaplan-Meier survival curve for WT BALB/c mice, (**E**) FcγR null BALB/c, or (**F**) WT BALB/c in the presence or absence of CD8$^+$ T cell depleting antibody (n=8-10, Mantel-Cox test).